INTERNATIONAL JOURNAL OF
MARITIME TECHNOLOGY

IJMT Vol.14/ Summer 2020 (21-32)

Available online at: www. ijmt.ir

Progressive Collapse Analysis of a Composite Ship Hull Girder under Vertical Bending using Finite Element Method

Sepideh Jafarzadeh[1], Mohammad Reza Khedmati[2*]

[1] *Graduated Master Student, Department of Maritime Engineering, Amirkabir University of Technology, Tehran 15916-34311, Iran, sepideh.jafarzadeh@ntnu.no*
[2] *Professor, Department of Maritime Engineering, Amirkabir University of Technology, Tehran 15916-34311, Iran, khedmati@aut.ac.ir*

ARTICLE INFO

Article History:
Received: 05 Nov. 2019
Accepted: 29 Sep. 2020

Keywords:
Composite ship hull girder
Vertical bending
Progressive failure
Ultimate strength
Finite Element Method (FEM)

ABSTRACT

This paper presents the collapse behaviour of a composite ship hull girder under vertical bending. Finite element method is used to provide valuable information regarding moment-curvature relationships and progressive failure characteristics of the composite ship hull girder. The analysis is carried out using ANSYS 12.0 finite element software. The response of the structure to the incrementally-increased sagging and hogging bending moments has been implemented and studied.

1. Introduction

Building ships in composite materials has been widely expanded in the recent years owing to the increasing demands for high-speed sea transportation. Compared with steel, lightweight materials such as composites enable the designers to achieve lightweight ship structures.

On the other hand, the length of composite ships has risen in the past years. As examples, reference may be made to some recently-built composite frigates and composite passenger ships. Increasing the length of the ship is meant to increase the amount of the vertical bending moment affecting the ship's structure cross-sections. This in turn increases probability of failure to the ship hull structure. Thus, having larger composite ships in length necessitates assessment of their ultimate bending strength in the early stages of structural design.

2. Literature review

The ultimate strength of steel ships has been broadly investigated by many researchers around the arena. Caldwell [1] became the first who anticipated the ultimate strength of steel ships using the fully plastic bending concept of the beams. However, he failed to take into account the reduction within the load-carrying capacity of structural members once they attain their corresponding ultimate strengths. Smith [2] proposed an approach for calculation of the ultimate strength of the ships. He initially divided the ship's cross section into various unstiffened/stiffened plate panels, and afterward performed a progressive collapse analysis under bending on it assuming that the cross section remains plane after bending while each of the panels behaves according to its corresponding average stress–average strain relationship. Finite element method was applied by Smith [2] in order to obtain the average stress–average strain relationships for unstiffened/stiffened panels. Derivation of the average stress-average strain relationships for ships' unstiffened /stiffened plate panels subject to in-plane compression alone or in combination with other loads using analytical approaches was tried by other researchers. Among them, reference may be made to the work of Khedmati [3].

Alongside above-mentioned research studies on the ultimate strength of the ships without considering the effect of the superstructure, some theoretical methods are also available to estimate the ultimate strength of the ship's hull with a superstructure mainly based on the simple beam theory or two-beam theory. The effect of superstructure on the longitudinal strength of a ship has been studied both experimentally and numerically by Mackney and Rose [4]. They applied simple beam theory and finite element method in their study, but ignoring the connection between the hull and superstructure. A new approach, which is called as the Coupled Beams Method (CBM), was proposed by Naar et al. [5] to evaluate the hull girder response of passenger ships. The main assumption in the CBM is that the global bending response of a modern passenger ship can be estimated by the help of beams coupled to each other by means of some distributed longitudinal and vertical springs. Naar et al. [5] also proposed an

analytical method in order to solve the governing equations when only the superstructure is as long as the ship's hull.

The ultimate strength of composite ships has been addressed in a very limited number of publications. Chen et al. [6] were the first who tried to estimate the ultimate strength of composite ships based on an analytical method, in which the behaviour of composite panels was being formulated with a simple formula. Chen and Soares [7] extended the above-mentioned method for calculating the ultimate strength of composite ships under bending moment, considering the panel buckling as well as fracture of the composite materials. Reliability analysis of composite ships under bending moment using the first method proposed by Chen et al. [6] was later performed by Chen and Soares [8]. To calculate the reliability of the reinforced plate buckling failure, the failure of the first layer of the reinforcing plate and the ultimate failure of the reinforced plate were considered.

Finally, Chen and Soares [9] implemented the conventional Smith's method in order to estimate the ultimate strength of composite vessels. Morshedsoluk and Khedmati [10] investigated the effect of the composite superstructures on the ultimate strength of the composite ships, following their work on the extension of the coupled beams method to study the ship's hull-superstructure interaction problems [11]. A simple analytical model to estimate the longitudinal strength of ship hulls in composite materials under buckling, material failure and ultimate collapse was also presented by Zhang et al. [12].

The behaviour of a composite vessel structure under incrementally-increased vertical bending moment is studied applying the finite element method in this study. Vertical bending moment is applied in both sagging and hogging conditions. Finally, the ultimate longitudinal strength of the composite hull, in both hogging and sagging conditions, is obtained from the moment–displacement relationship, which is established by imposing progressively increasing load on the hull girder. The results may be useful as a benchmark study for further investigations.

3. Description of the vessel

The vessel under consideration in this study is fully made of composite materials and longitudinally framed. Length, breadth and depth of the vessel are 50 meters, 9 meters and 6 meters, respectively [9].

The plates in structure of the vessel are stiffened with hat-type stiffeners. A view on the half of the midship section of the vessel is shown in Figure 1 [9]. Stacking sequence of the composite layers of plate, stiffener's web, stiffener's flange and table of stiffened plates at deck and side shell regions are $[0_4/45/0_4/45]_s$, $[0_4/45/0_4/45]_s$, $[0_4/45/0_4/45]_s$ and $[0_5/45/0_5/45]_s$, respectively. On the other hand, stiffened plates at the bilge and bottom regions have the stacking sequence as $[0_6/45_2/0_6/45]_s$, $[0_6/45_2/0_6/45]_s$, $[0_6/45_2/0_6/45]_s$ and $[0_7/45_2/0_7/45]_s$, respectively for plate, stiffener's web, stiffener's flange and table parts. Geometrical details and dimensions of the stiffened plates in the composite ship are given in Figure 2 [9] and Table 1 [9]. Properties of the WR/polyester GRP material used for the ship construction are also described in Table 2 [9].

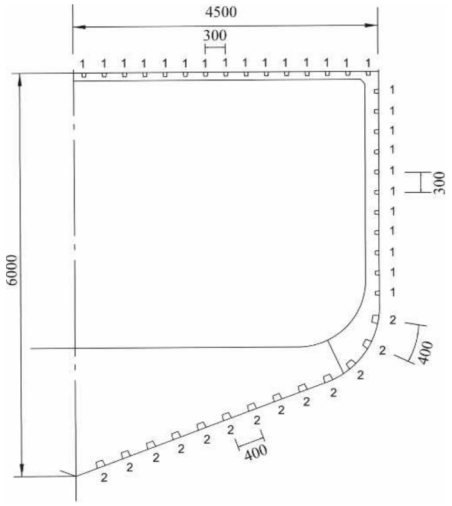

Figure 1. Half of the midship section of the composite ship (Dimensions in *mm*) [9].

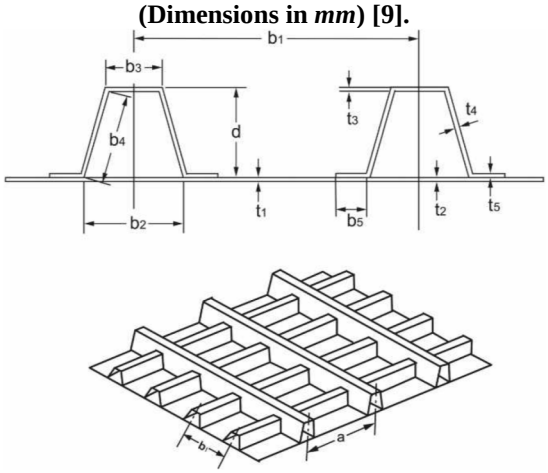

Figure 2. Geometrical details of the stiffened plates in deck, side shell and bilge of the composite ship [9].

Table 1. Geometrical dimensions of the stiffened plates in the composite ship in *mm* [9].

Item	*a*	b_1	b_2	b_3	b_4	b_5	t_1,t_2,t_4,t_5	t_3	*d*
Deck and Side Shell	1000	300	62	50	57.3	18	10	12	60
Bilge	1000	400	124	100	84.8	38	15	17	90

Table 2. Properties of the WR/polyester GRP material [9].

Property	Symbol	Value
Elastic modulus in 1 principal material direction	E_1	15.8 *GPa*
Elastic modulus in 2 principal material direction	E_2	15.8 *GPa*
Shear modulus in 1-2 and 1-3 principal material planes	G_{12},G_{13}	3.5 *GPa*
Shear modulus in 2-3 principal material plane	G_{23}	0.35 *GPa*
Poisson's ratio	v_{12}	0.13
Tensile strength in 1 principal material direction	X_T	249 *MPa*
Compressive strength in 1 principal material direction	X_C	213 *MPa*
Tensile strength in 2 principal material direction	Y_T	249 *MPa*
Compressive strength in 1 principal material direction	Y_C	213 *MPa*
Shear strength in 1-2 principal material plane	R	104 *MPa*
Shear strength in 2-3 principal material plane	S	23.5 *MPa*
Shear strength in 1-3 principal material plane	T	23.5 *MPa*

4. Finite element analysis

The finite element analyses are carried out using version 12.0 of commercial software ANSYS [13]. Some detailed information on the finite element analyses are given below.

4.1. Extent of the model

It should be noted that at first, only a half of the section of the vessel was modelled, while symmetry condition was imposed on the longitudinal centre plane of the vessel. However, some problems with convergence were noticed during the analysis with the consideration of symmetry. The reason for this was the presence of some layers with stacking angles other than 0 and 90 degrees in the composite ship construction. In other words, the condition of symmetry in addition to illustrating the geometry of the model on the other side also depicts the angles of composite layer fibres. For example, if the angle of the fibres in a layer located on the right-side of the section is equal to 45 degrees, then when the symmetry is considered, the angle of fibres of that layer in the left-side region of the model will change to -45 degrees. That is why, the entire section of the vessel, as shown in Figure 3, was finally modelled.

The composite ship under consideration is 50 meters long. Obviously, whole ship hull is not resisting against vertical bending. In fact, the parallel middle body of the ship is mainly contributing to its ultimate longitudinal strength under vertical bending. Accordingly, a selected region of the ship's parallel middle body is considered as the test section in the numerical four-point bending setup shown in Figure 4. It has been revealed that such a methodology fulfills well the longitudinal vertical bending conditions of the ship's hull in real practice [14].

In order to assess the collapse behaviour of the composite ship hull under consideration herein, a 15-meter-long model is created. An overall view on the model of the composite ship is shown in Figure 4. Test section, each of buffer sections and also each of outer sections have a length of 3 meters, 1 meter and 5 meters, respectively.

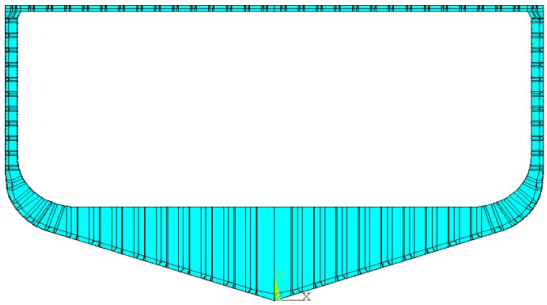

Figure 3. Section of the composite ship.

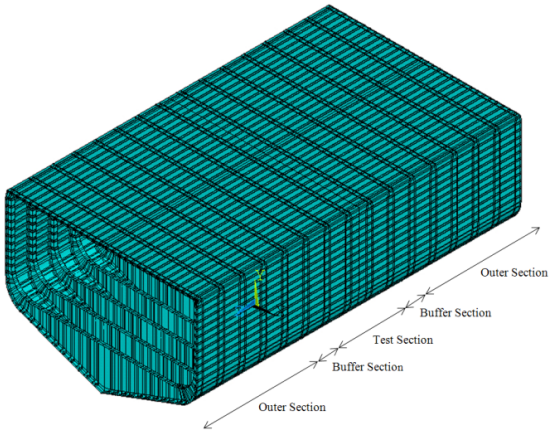

Figure 4. Overall view on the model of the composite ship.

The principle of four-point bending setup is schematically depicted in Figure 5. The test section in middle is surrounded by two buffer sections and two outer sections, in a symmetrical way. No shear force is created in the central span of the setup, while a pure uniform bending moment acts there. The buffer sections and also the outer sections accommodate some kind of strengthened transverse ring frames or transverse diaphragms to transfer the transverse loads. Besides, the outer sections act as the arms in the four-point bending setup.

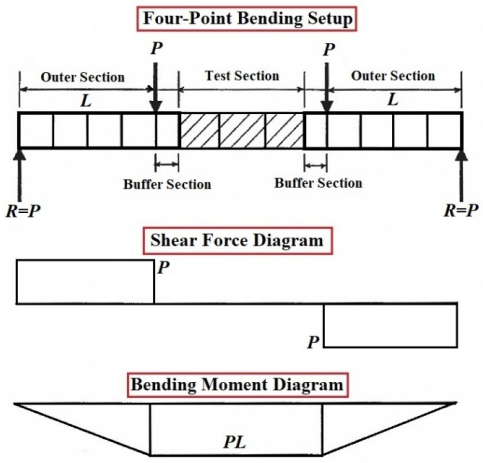

Figure 5. Four-point bending setup.

As it was shown earlier in Figure 1, longitudinal stiffeners are of hat type anywhere in the composite ship. Transverse frames in the bottom region of the vessel are of tee type, while they are of hat type elsewhere. Some snapshots on the modelled geometries of different regions and connections are depicted in the Figures 6 to 11. Figure 12 demonstrates a zoomed-in view of the inside of the composite ship hull model.

The connections between deck, side, bottom and corresponding stiffening elements such as longitudinal stiffeners and transverse frames are defined at the event of creating the geometry. In other word, all intersecting areas of the model are divided and partitioned and then, they are merged together so that a common line is created at the junction of the intersecting areas. In this way, at the time of meshing the geometry, all intersecting areas would have common nodes.

Scantlings of structural elements in both buffer sections and outer sections compared with those in the test section are so increased or strengthened that the onset of progressive collapse locates only in the test section. In other words, the buffer sections and also the outer sections remain intact at the end of numerical or experimental four-point bending. This is due to the fact that capturing or exploiting the collapse features of the test section is the main target in the four-point bending setup.

Thicknesses given in Table 1 are used for corresponding parts in the test section. Besides, thickness of each part located in the buffer or outer sections of the model is obtained from the thickness given in Table 1 but multiplied by 5. Stacking sequences for the layers are exactly the same as those explained above.

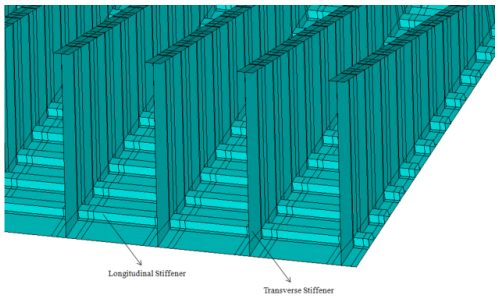

Figure 6. A zoomed-in view of the modelled bottom of the composite ship.

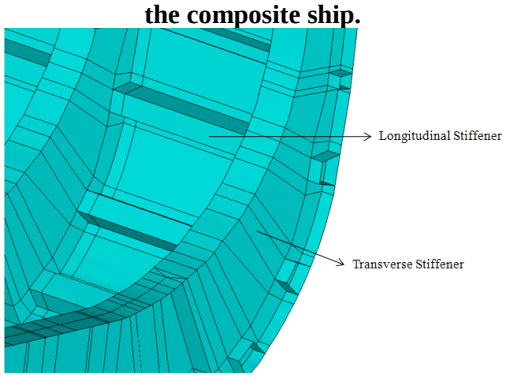

Figure 7. A zoomed-in view of the modelled bilge of the composite ship.

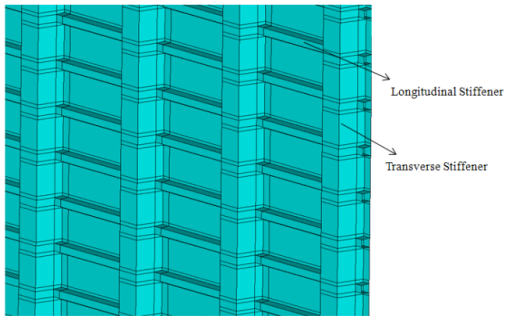

Figure 8. A zoomed-in view of the modelled side shell of the composite ship.

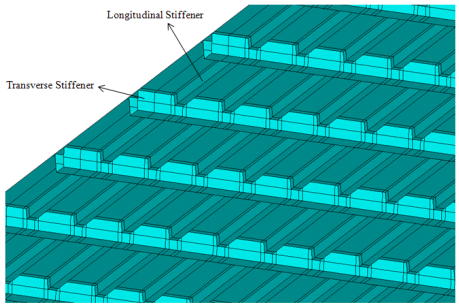

Figure 9. A zoomed-inside view of the modelled deck of the composite ship.

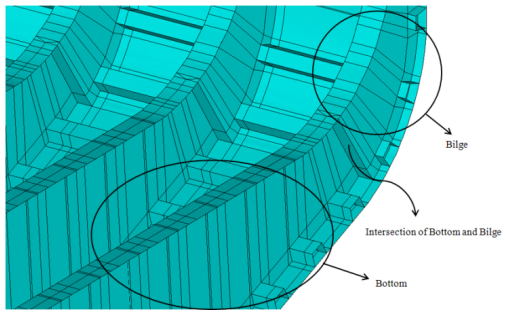

Figure 10. A zoomed-in view of the bottom-to-bilge connection of the composite ship.

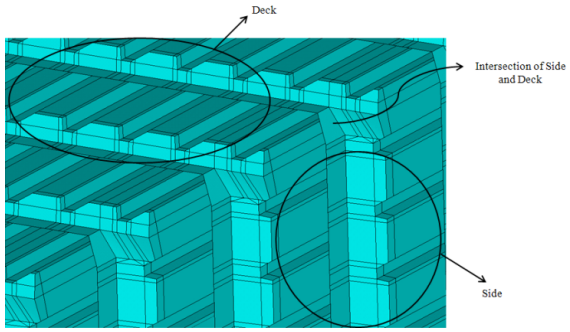

Figure 11. A zoomed-inside view of the deck-to-side shell connection of the composite ship.

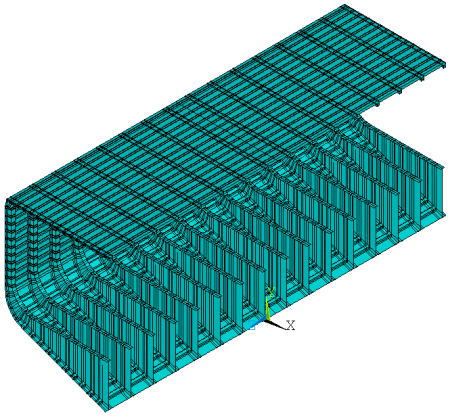

Figure 12. A zoomed-in view of the inside of the composite ship hull model.

4.2. Mesh generation

Different parts of the model including plates, longitudinal stiffeners and transverse frames are all discretised using the layered SHELL281 elements, Figure 13. This type of finite element (available in the element library of ANSYS) can be used for analysing thin to moderately thick shell structures. The element has 8 nodes with 6 degrees of freedom per each of the nodes (translations along x, y and z axes together with rotations about x, y and z axes). It is used for linear as well as nonlinear analyses. In addition, it is possible to consider the variation in shell thickness in nonlinear analyses. SHELL281 elements are suitable for modelling layered structures such as composites and sandwich systems. It should also be noticed that the accuracy of the SHELL281 elements when modelling composites is based on the First-order Shear Deformation Theory.

Figure 14 shows the discretised composite ship hull model. Density of the mesh is increased in the test section of the model. A number of 83907 elements in total have been employed to construct the finite element model. Table 3 represents the details on the distribution of finite elements used for discretisation of the model.

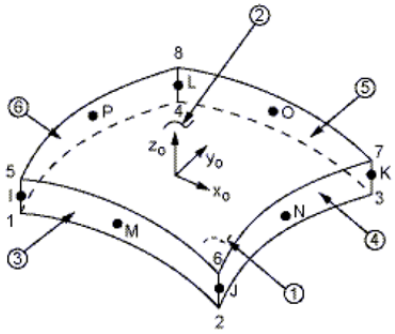

Figure 13. ANSYS SHELL281 element used for discretisation of the composite ship hull model.

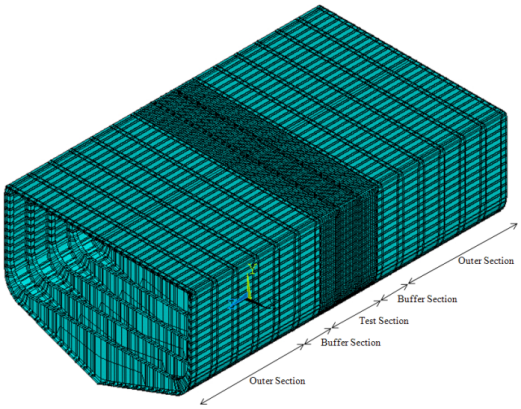

Figure 14. Discretised composite ship hull model.

Table 3. Distribution of finite elements used for discretisation of the model.

Item	Quantity	No. of Elements/Quantity	Total No. of Elements
One meter of test section	3	10825	32475
One meter of buffer section	2	4286	8572
One meter of outer section	10	4286	42860
Sum			83907

4.3. Initial imperfections

It is clear that the initial imperfections are influencing the bending behaviour and ultimate strength of the structure under consideration. Study of the amounts of such influential effects has not been the main goals of this investigation. That is why, no initial imperfection has been accounted for within the finite element models created and analysed herein.

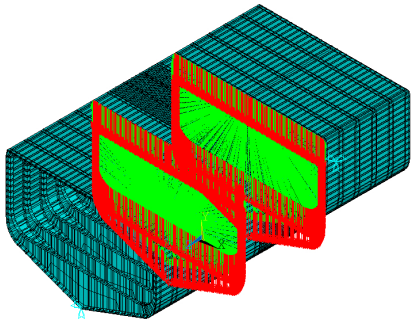

(a) sagging condition

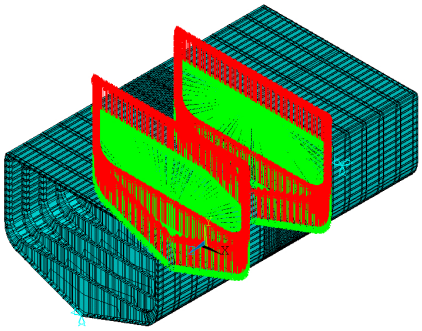

(b) hogging condition

Figure 15. Loading and boundary conditions imposed on discretised composite ship hull model.

4.4. Boundary and loading conditions

Behaviour of the finite element model shown in the Figure 14 has been evaluated under both sagging and hogging conditions of vertical bending. A four-point numerical bending setup is created on the model. Displacements of the nodes located on the lowermost edge of the right-hand-side face of the model (Figure 14) along all three axes (x, y and z) are restrained. On the other hand, for the nodes placed on the lowermost edge of the left-hand-side face of the model (Figure 14), restraining is performed just along x and y axes.

In sagging condition, two equal downward forces each with the amount of 37800000 *N* are incrementally distributed on two transverse frames located at a distance of 1 meter from both ends of the test section. On the other hand, two equal upward forces each with the amount of 55500000 *N* are incrementally distributed on the same two transverse frames mentioned above, for the case of hogging condition. In such a way, the test section of the model is subjected to pure bending. Loading and boundary conditions imposed on discretised composite ship hull model in both sagging and hogging conditions are shown in the Figures 15(a) and 15(b), respectively.

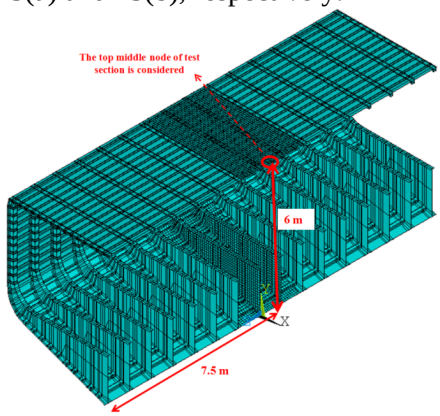

Figure 16. Position of the reference point where variation of its vertical displacement versus variation of the bending moment is demonstrated in a curve.

4.5. Simulation of progressive bending process

Nonlinear analyses are performed on the created finite element model. Both material and geometric nonlinearities are taken into consideration. The relationship between vertical bending moment applied on the model and vertical displacement of a reference point (where its location is shown in Figure 16) is traced throughout the analyses. In addition to the reference point, a selection of other complementary points (Figure 17) located in the test section of the composite ship hull model is also specified in order to extract the trends of their (vertical or horizontal) displacements versus bending moment. The main results are moment-displacement curve accompanied with a history of deflection/stress contours originated from the start of loading and leading to the final collapse of the model. The results are summarised in both sagging and hogging conditions.

In order to simulate the process of progressive bending, the downward/upward forces are incrementally applied on the transverse frames. Adopted numbers of load steps, substeps and equilibrium iterations in each substep are considered to be 1, 50 and 15, respectively. Beside taking the option of "static large displacements" into account in the analyses, the arc-length method is also activated with the minimum and maximum multipliers set at the values of 0.001 and 10, respectively. The maximum displacement of vertical displacement of the reference point is also assumed to be 0.5 meter for controlling the end of analyses.

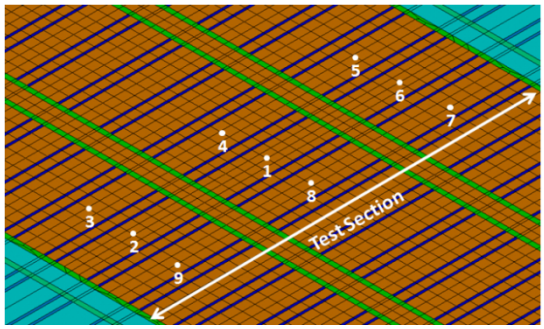

(a) in the deck region

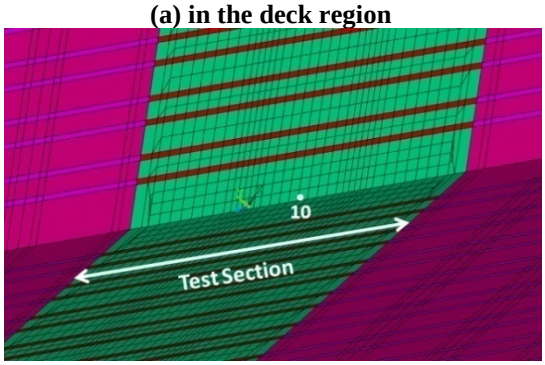

(b) in the bottom region

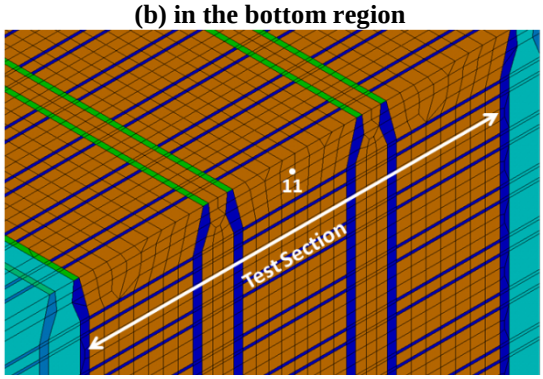

(c) in the side shell region

Figure 17. Position of selected complementary points in the test section of the composite ship hull model, for drawing the curves of bending moment versus their (vertical or horizontal) displacements.

5. Analysis

Analyses are performed on a personal computer with 4.00 GB RAM and Intel Core 2 Duo CPU (E7400) at 2.80 *GHz* running on MS Windows XP Service Pack 2 operating system [15]. Each of the analyses takes approximately a period of 160 to 180 hours of time.

5.1. Failure identification

Tsai-Wu criterion is employed in order to identify any failure of the composite materials within the finite element model. Failure index (F) is defined in the following form in the adopted Tsai-Wu failure criterion:

$$F \equiv F_1\sigma_1 + F_2\sigma_2 + F_3\sigma_3 + F_{11}\sigma_1^2 + F_{22}\sigma_2^2 + F_{33}\sigma_3^2 + 2F_{12}\sigma_1\sigma_2 + 2F_{13}\sigma_1\sigma_3 + 2F_{23}\sigma_2\sigma_3 + F_{44}\sigma_{12}^2 + F_{55}\sigma_{23}^2 + F_{66}\sigma_{13}^2 \quad (1)$$

Where

$$F_1 = \frac{1}{X_T} - \frac{1}{X_C}, F_2 = \frac{1}{Y_T} - \frac{1}{Y_C}, F_3 = \frac{1}{Z_T} - \frac{1}{Z_C},$$

$$F_{11} = \frac{1}{X_T X_C}, F_{22} = \frac{1}{Y_T Y_C}, F_{33} = \frac{1}{Z_T Z_C},$$

$$F_{12} = -\frac{1}{2\sqrt{X_T X_C Y_T Y_C}}, F_{13} = -\frac{1}{2\sqrt{X_T X_C Z_T Z_C}}, F_{23} = -\frac{1}{2\sqrt{Y_T Y_C Z_T Z_C}},$$

$$F_{44} = \frac{1}{R^2}, F_{55} = \frac{1}{S^2}, F_{66} = \frac{1}{T^2}$$

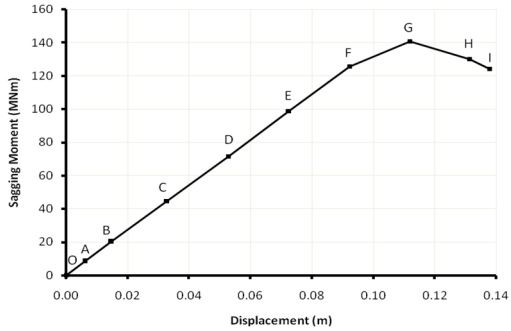

(a) bending moment versus vertical displacement (at reference point) curve

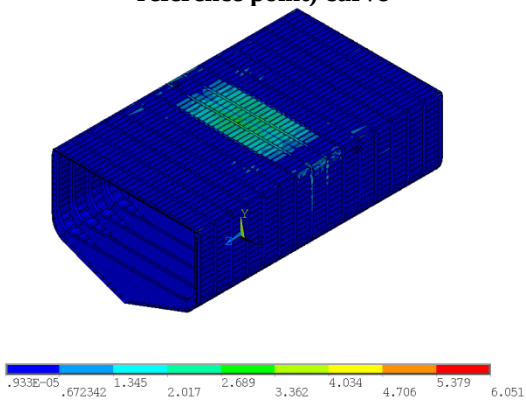

(b) distribution of Tsai-Wu criterion index in the composite ship hull model, at point I of the bending moment - vertical displacement curve

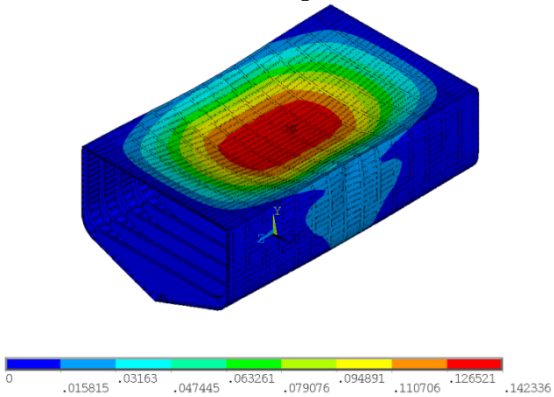

(c) deflection the composite ship hull model, at point I of the bending moment - vertical displacement curve

Figure 18. Results for the sagging condition.

In above relations, σ_i represents stress component along the principal material coordinate i (i=1, 2, 3). X_T, Y_T and Z_T are the lamina normal strengths in tension along material coordinates, X_C, Y_C and Z_C are the lamina normal strengths in compression along material coordinates. In addition, R, S and T are the lamina shear strengths in the material planes 1-2, 2-3 and 1-3, respectively. It should be noted that failure happens when $F \geq 1$.

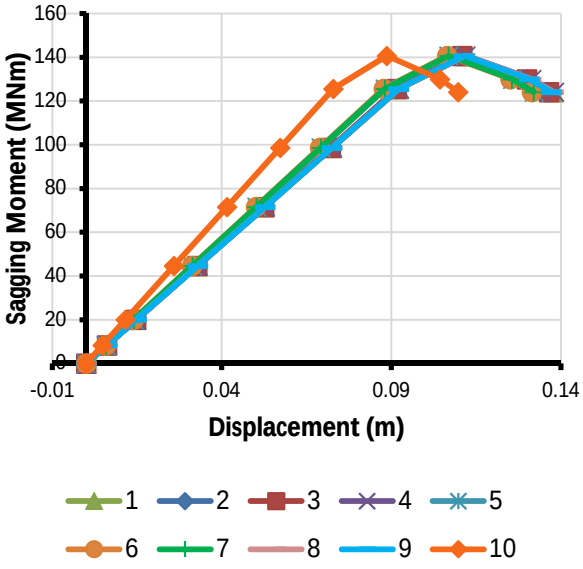

(a) deck/bottom regions (vertical displacement)

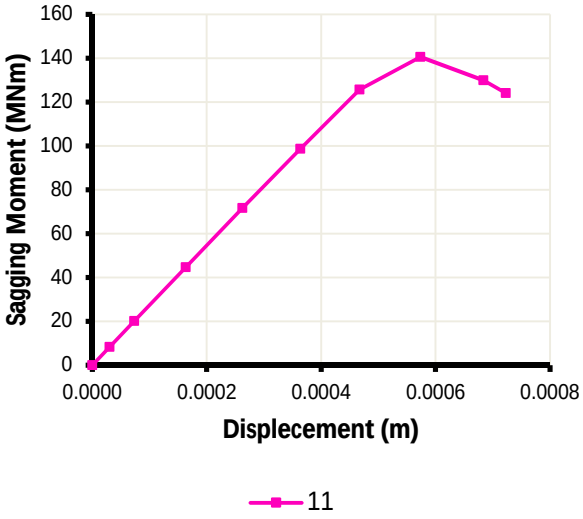

(b) side shell region (horizontal displacement)

Figure 19. Variations of sagging (bending) moment versus (vertical or horizontal) displacement at selected complementary points of the test section of the composite ship hull model.

5.2. Sagging condition

Results for the sagging condition are summarised in Figure 18. Based on the moment-vertical displacement (at reference point) curve shown in Figure 18(a), the ultimate vertical sagging bending moment carried by the composite ship hull model is 140.67 *kN.m*. Figures

18(b) and 18(c) demonstrate distribution of Tsai-Wu criterion and deflection pattern in the composite ship hull model, respectively but both at final step of calculations (specified by point I on the curve shown in Figure 18(a)). Variations of sagging (bending) moment versus (vertical or horizontal) displacement at selected complementary points of the test section of composite ship hull model are also shown in Figure 19.

Progressive distribution of Tsai-Wu criterion index and deflection in the deck region of the composite ship hull model, at different points of the sagging bending moment-vertical displacement curve are gathered in Tables 4 and 5, respectively.

Table 4. Distribution of Tsai-Wu criterion index in the deck region of the composite ship hull model, at different points of the sagging bending moment - vertical displacement curve.

Point	Sagging Moment (*MN.m*)	Equivalent Tsai-Wu Index Contours
O	2.70	
A	8.34	
B	20.10	
C	44.66	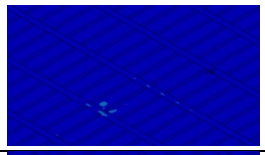
D	71.64	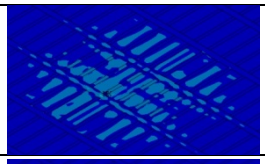
E	98.64	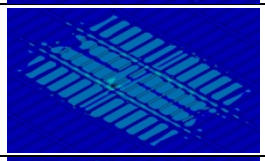
F	125.64	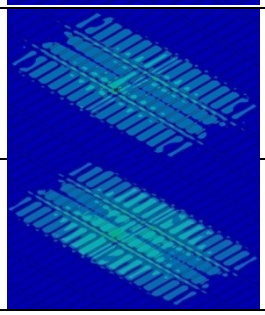
G	140.66	
H	130.00	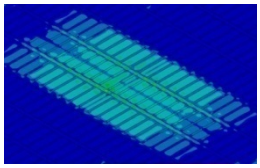
I	124.11	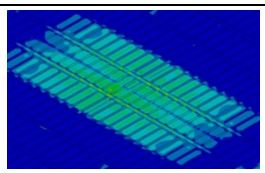

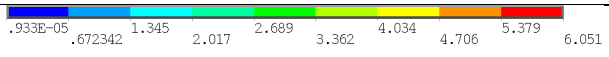

Table 5. Deflection of the deck region of the composite ship hull model, at different points of the sagging bending moment - vertical displacement curve.

Point	Sagging Moment (*MN.m*)	Equivalent Displacement Contours
O	2.70	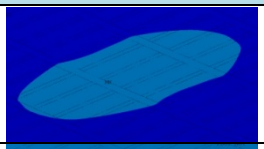
A	8.34	
B	20.10	
C	44.66	
D	71.64	
E	98.64	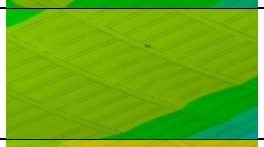
F	125.64	
G	140.66	
H	130.00	
I	124.11	

5.3. Hogging condition

Results for the hogging condition are summarised in Figure 20. Based on the moment-vertical displacement (at reference point) curve shown in Figure 20(a), the ultimate vertical hogging bending moment carried by the composite ship hull model is 200.00 *kN.m*. Figures 20(b) and 20(c) demonstrate distribution of Tsai-Wu criterion and deflection pattern in the composite ship hull model, respectively but both at final step of

calculations (specified by point G on the curve shown in Figure 20(a)). Variations of hogging (bending) moment versus (vertical or horizontal) displacement at selected complementary points of the test section of composite ship hull model are also shown in Figure 21. Progressive distribution of Tsai-Wu criterion index and deflection in the deck region of the composite ship hull model, at different points of the hogging bending moment - vertical displacement curve are gathered in Tables 6 and 7, respectively.

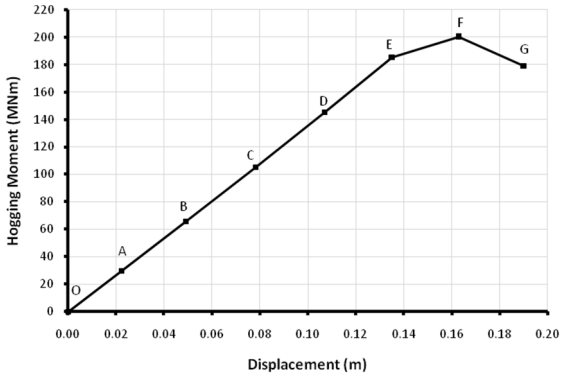

(a) bending moment versus vertical displacement (at reference point) curve

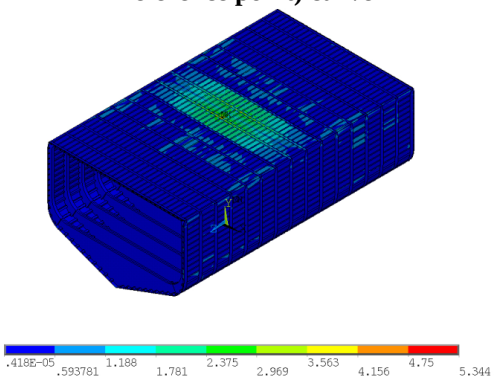

(b) distribution of Tsai-Wu criterion index in the composite ship hull model, at point G of the bending moment - vertical displacement curve

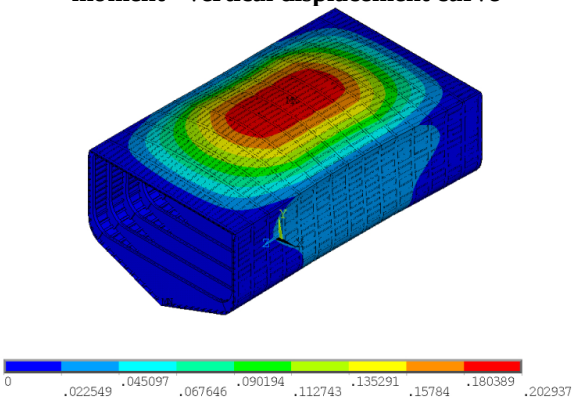

(c) deflection the composite ship hull model, at point G of the bending moment - vertical displacement curve

Figure 20. Results for the hogging condition.

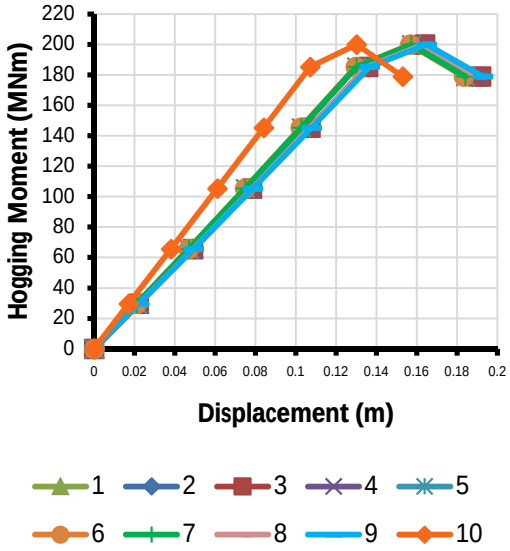

(a) deck/bottom regions (vertical displacement)

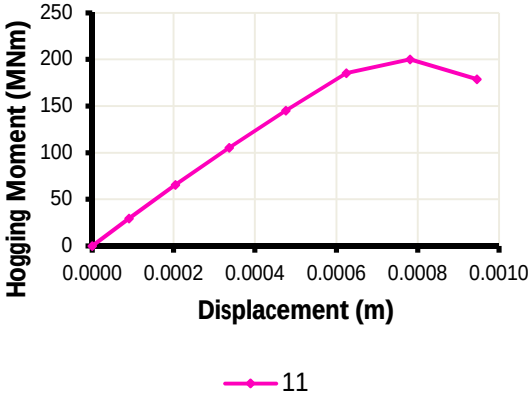

(b) side shell region (horizontal displacement)

Figure 21. Variations of hogging (bending) moment versus (vertical or horizontal) displacement at selected complementary points of the test section of the composite ship hull model.

6. Verification and discussions

Since no experimental results are available concerning the ultimate strength of the composite ship hulls in bending, the results of finite element analyses reported above are verified against the results obtained by Chen and Soares [7 and 9]. Tables 8 and 9 together with Figure 22 explain the verification results. It should be mentioned that the studies made by Chen and Soares [7 and 9] do not provide any information regarding the moment-displacement curves, while they are mainly focused on estimation of the value of ultimate strength. In contrast, full-range moment-displacement curves can be obtained from the finite element analysis for the composite ship hull under either sagging or hogging condition of vertical bending. Figure 22 in addition to the Tables 8 and 9 confirm the fact that the values of ultimate strength of the composite ship hull under consideration as obtained by the present finite element analyses are in near consistency with those obtained by Chen and Soares [7 and 9].

Table 6. Distribution of Tsai-Wu criterion index in the deck region of the composite ship hull model, at different points of the hogging bending moment - vertical displacement curve.

Point	Hogging Moment (*MN.m*)	Equivalent Tsai-Wu Index Contours
O	3.96	
A	29.53	
B	65.65	
C	105.41	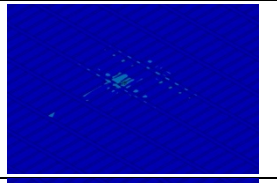
D	145.25	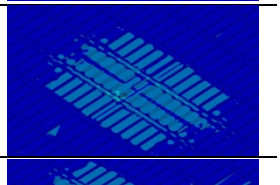
E	185.18	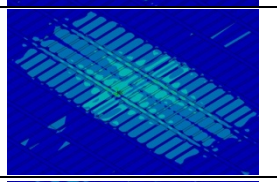
F	200.00	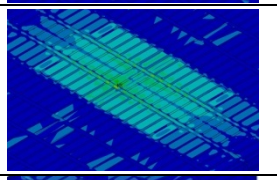
G	178.99	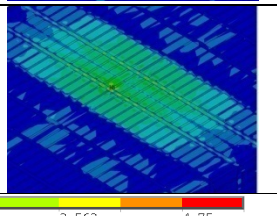

Structural behaviour of the composite ships is complex due to the non-isotropic nature of the composites. The modulus of elasticity of the composite materials used in shipbuilding industry is usually much less than the corresponding value of shipbuilding steels. Hence, the composite plates constructing the structure of the ships are more prone to buckling. Brittleness of the composite materials not only causes the material to fail in the local areas of the ship, but also leads to the reduction of the residual strength of the composite plates. Under sagging bending of the hull, the deck is compressed while the bottom is tensioned. Compressive strength of the composite materials is less than its tensile strength. In this way, the deck plates are buckled. As the load is further increased, the plates exhibit their post-buckling behaviours. With exceeding the value of failure index from the limit value of 1, brittle failure happens and spreads inside their different layers. Failure of the composite plates in deck structure results in the collapse of the deck, followed by the collapse of the entire ship structure.

Table 7. Deflection of the deck region of the composite ship hull model, at different points of the hogging bending moment - vertical displacement curve.

Point	Hogging Moment (*MN.m*)	Equivalent Displacement Contours
O	3.96	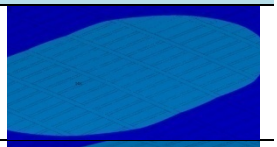
A	29.53	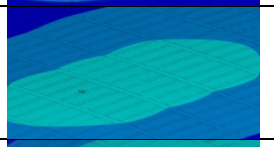
B	65.65	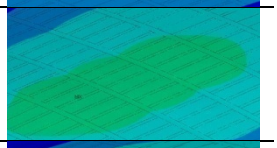
C	105.41	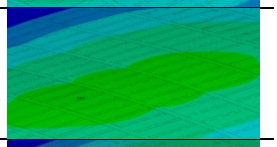
D	145.25	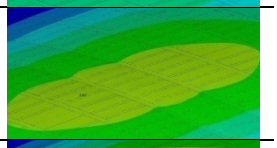
E	185.18	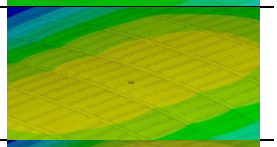
F	200.00	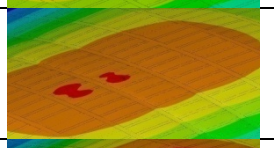
G	178.99	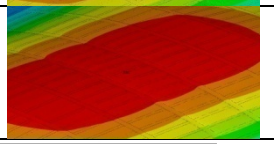

(m)

In the hogging mode of bending, the deck is under tension while the bottom is under compression. Due to the lower compressive strength of the composite material in comparison with its tensile strength, it is expected that first the bottom of the ship structure buckles. But contrary to expectations, the deck plates are failed. The reason for this is the lack of geometric similarity between the deck and the bottom and moreover, existence of rise of floor in the bottom region. In composite ships with non-zero angles of rise of floor, due to the concentration of the pressures on the bottom structure, the structure of this part of the ship has highly strong components to the effective loads. Therefore, in general, the structure of the bottom of this category of ships is stronger than the structure of their decks. Thus, in this situation, the neutral axis is closer

to the bottom, and subsequently the probability of a tensile or compression failure in the deck is increased in both hogging and sagging modes of bending. It is expected that with the decrease in the floor angle, failure will occur in other areas of this type of ships.

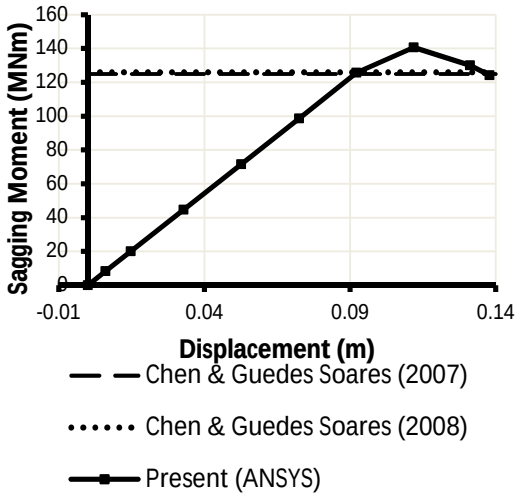

(a) sagging condition

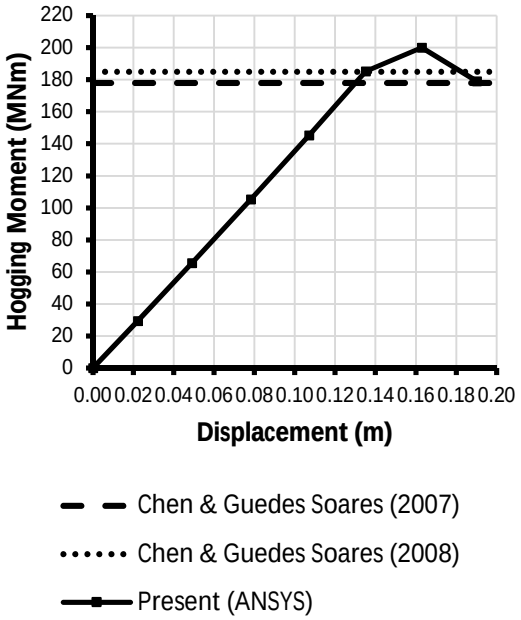

(b) hogging condition

Figure 22. Comparison of the results.

Table 8. Comparison of the results for sagging condition.

Method	Chen & Guedes Soares (2008)	Chen & Guedes Soares (2007)	Present (ANSYS)
Ultimate Moment (*kN.m*)	126	125	140.67
Initial Residual Stresses	×	×	×
Initial Geometric Imperfections	×	×	×
Error with respect to Chen & Guedes Soares (2008) (%)	-	0.8	11.64

Table 9. Comparison of the results for hogging condition.

Method	Chen & Guedes Soares (2008)	Chen & Guedes Soares (2007)	Present (ANSYS)
Ultimate Moment (*kN.m*)	185	178	200.00
Initial Residual Stresses	×	×	×
Initial Geometric Imperfections	×	×	×
Error with respect to Chen & Guedes Soares (2008) (%)	-	3.8	8.11

7. Conclusions

In this paper, progressive bending of a composite ship hull is simulated with the aid of the finite element method. The finite element model of the composite ship hull is subjected to pure bending in two modes of sagging and hogging. By performing nonlinear analyses on this model, its longitudinal ultimate strength was assessed in both sagging and hogging modes. Finally, the results of these simulations were compared with the results of other researchers. The comparison showed that the ultimate strength obtained by the finite element method in the present study is in agreement with other results. The main reasons behind differences of the obtained results are:

1) *Lack of access to the body lines and actual shape of the ship:* The only available information on the geometry of this vessel is including the section shown in Figure 1, length, breadth, and height of the ship, and the values given in Table 1. In the event of access to more specific and accurate specifications, the error is reduced.

2) *The lack of access to the full details of the material:* The existing information on the properties of the materials, as outlined in Table 2, is incomplete. The values of the modulus of elasticity in relation to the main material direction 3, the Poisson's ratio in the main material surfaces 1-3 and 2-3, and the tensile/compressive strengths in main material direction 3 are not specified. These unknowns are determined using the micromechanics relationships.

3) *Adoption of a limited number of incremental steps:* Due to the lengthy time of the nonlinear analyses, applying the desired force in a larger number of steps and increasing the accuracy of the solution is not possible. Of course, more accurate results may be expected by means of parallel processing systems.

Acknowledgements

The research reported in this paper are extracted from the results obtained in the MSc studies of the first author under supervision of the second author in the Department of Maritime Engineering of Amirkabir University of Technology in Tehran, Iran [15].

Funding

The authors received no financial support for the research, authorship, and/or publication of this article.

References

1- Caldwell, J.B., (1965), *Ultimate longitudinal strength*. Trans RINA; 207:411-430.
2- Smith, C.S., (1977), *Influence of local compressive failure on ultimate longitudinal strength of a ship's hull*. In: Proc Int Symp on Practical Design in Shipbuilding, Tokyo, Japan, p. 73–9.
3- Khedmati, M.R., (2005), *Simulation of average stress average strain relationship of ship unstiffened /stiffened plates subject to in plane compression*. Scientia Iranica; 12 (4): 359-367.
4- Mackney, M.D.A., Rose, C.T.F., (1999), *Preliminary ship design using one-and two-dimensional models*. Marine Technology; 36(2):102-111.
5- Naar, H., Varsta, P., Kujala, P., (2004), *A theory of coupled beams for strength assessment of passenger ships*. Marine Structures; 17(8):590-611.
6- Chen, N.Z., Sun, H.H., Guedes Soares, C., (2003), *Reliability analysis of a ship hull in composite material*. Composite Structures; 62(1):59-66.
7- Chen, N.Z., Guedes Soares, C., (2007), *Longitudinal strength analysis of ship hulls of composite materials under sagging moments*. Composite Structures; 77(1):36-44.
8- Chen, N.Z., Guedes Soares, C., (2007), *Reliability analysis of ship hulls made of composite materials under sagging moments*. Journal of Marine Science and Technology; 12(4):263-271.
9- Chen, N.Z., Guedes Soares, C., (2008), *Ultimate longitudinal strength of ship hulls of composite materials*. Journal of Ship Research; 52(3):184-193.
10- Morshedsolouk, F., Khedmati, M.R., (2016), *Ultimate strength of composite ships' hull girders in the presence of composite superstructures*. Thin-Walled Structures; 102:122-138.
11- Morshedsolouk, F., Khedmati, M.R., (2011), *An extension of coupled beam method and its application to study ship's hull-superstructure interaction problems*. Latin American Journal of Solids and Structure; 8(3):265-290.
12- Zhang, X., Huang, L., Zhu, L., Tang, Y., and Wang, A., (2017), *Ultimate longitudinal strength of composite ship hulls*. Curved and Layered Structures; 4(1):158-166.
13- Swanson Analysis Systems Inc., *ANSYS user's manual* (Version 12.0). Houston.
14- Hughes, O.F., Paik, J.K., (2010), *Ship Structural Analysis and Design*. The Society of Naval Architects and Marine Engineers (SNAME), USA.
15- Jafarzadeh, S., (2011), *Modelling and evaluation of ultimate strength of composite ships using finite element method*. MSc Thesis (supervised by Dr. Mohammad Reza Khedmati), Amirkabir University of Technology, Tehran, Iran.